PHOTODESTRUCTION OF RELEVANT INTERSTELLAR MOLECULES IN ICE MIXTURES

Hervé Cottin

Laboratoire Interuniversitaire des Systèmes Atmosphériques, Universités Paris VII-Paris XII, Créteil, France; cottin@lisa.univ-paris12.fr

Marla H. Moore

Astrochemistry Branch, Code 691, NASA Goddard Space Flight Center, Greenbelt, MD 20771; marla.h.moore@nasa.gov

and

Yves Bénilan

Laboratoire Interuniversitaire des Systèmes Atmosphériques, Universités Paris VII-Paris XII, Créteil, France;
benilan@lisa.univ-paris12.fr

ABSTRACT

UV photodestruction of some interstellar molecules is studied in different kinds of ices. CH_4, CH_3OH, NH_3, CO_2, CO, and HNCO are photolyzed as pure ices, or mixed with water or molecular nitrogen, at about 10 K. The destruction cross sections of these molecules are estimated for use in photochemical models of interstellar ices. We show that the destruction rate depends on the ice in which the studied compound is embedded.

Subject Headings: astrochemistry — ISM: molecules — methods: laboratory — molecular processes — ultraviolet: ISM

1. INTRODUCTION

Laboratory studies attempting to mimic interstellar ices, through the irradiation of low-temperature ice mixtures, have mainly been devoted to the study of complex organic molecules synthesized from a simple starting material, and contained in the refractory residue resulting from samples warmed to room temperature (see, e.g., Allamandola, Sandford, & Valero 1988; Schutte, Allamandola, & Sandford 1993; Bernstein et al. 1995; Dworkin et al. 2001; Cottin, Gazeau, & Raulin 1999 for a review of those experiments). But little is known about intrinsic chemical mechanisms dominating the evolution of simple ice mixtures, or about kinetic constants that are necessary to extrapolate laboratory simulations to interstellar environments. First steps toward a systematic approach have been published by Gerakines, Schutte, & Ehrenfreund (1996), who studied UV processing of pure ices and gave an exhaustive list of photoproducts and photodestruction cross sections. A comparison of UV photolysis and ion irradiation of CH_4 and CH_3OH is reported by Baratta, Leto, & Palumbo (2002), and CO is discussed by Gerakines & Moore (2001). Concerning binary mixtures, which are the next stage for understanding the ice chemistry, systematic studies have been performed on $H_2O + CO_2$ mixtures (Gerakines, Moore, & Hudson 2000), where the influence of photons versus protons is compared. Products, G values, and chemical mechanisms have been published for proton-irradiated mixtures such as $H_2O + CH_4$, $H_2O + C_2H_2$ (Moore & Hudson 1998), $H_2O + CO$, and $H_2O + H_2CO$ (Hudson & Moore 1999). More recently, Ehrenfreund et al. (2001) published the UV photodestruction rate of amino acids in H_2O, N_2, and Ar matrices, and Watanabe et al. (2002) measured the conversion rate of CO to CO_2 in H_2O ice.

The present paper focuses on the photodestruction rates of some of the most abundant molecules detected in interstellar medium ices: CO (Ehrenfreund et al. 1997),

CO_2 (Gerakines et al. 1999), NH_3 (Lacy et al. 1998), CH_4 (Boogert et al. 1998), and CH_3OH (Gibb et al. 2000). HNCO is also included in our study. Although not detected directly in interstellar ices, this molecule is present in the gas phase (Snyder & Buhl 1972; Jackson, Armstrong, & Barrett 1984) and in comets (Lis et al. 1997a, 1997b). HNCO is the simplest molecule containing all four atoms, H, N, C, and O. This paper contains the photodestruction of these six molecules as single-component ices, and also in polar (H_2O) and apolar (N_2) matrices.

In the first section, we present our experimental setup, with a focus on the estimation of the UV lamp flux, a critical parameter to derive quantitative photolysis data. Then we discuss some theoretical aspects of photolysis in ices, how it can be modeled, and how results such as the ones we present in this paper can be interpreted. Then we present our results, showing that the photodestruction rate may depend on the molecule's direct environment, i.e., the dominant ice molecule.

2. EXPERIMENTAL

2.1. *Ice Preparation and Analysis*

The experimental setup has been described in detail by Hudson & Moore (1995) and Moore & Hudson (1998, 2000). Basically, a gas mixture is condensed at a rate of ~3–5 μm hr^{-1} onto an aluminum cold mirror ($T < 20$ K) in a vacuum chamber ($P \sim 10^{-8}$ torr). The ice thickness is determined by measuring laser interference fringes during deposition. Ice films can be photolyzed with a UV lamp (described in the next section) and analyzed by infrared spectroscopy (each spectrum collected had 60 scans at 4 cm^{-1} between 4000 and 400 cm^{-1}). The photolysis of CH_4, CH_3OH, NH_3, CO_2, CO, and HNCO have been studied in pure form, and as a binary mixture dominated by N_2 or H_2O with a 10 : 1 ratio.

Gas-phase mixtures are made in a glass bulb in which the concentration of each component is determined by its partial pressure. The sources and purities of the compounds used are: triply distilled H_2O with a resistance greater than 10^7 ohm cm; N_2, Matheson research grade, 99.995%; CO, Matheson research grade, 99.99%; CO_2, Matheson research grade, 99.995%; CH_4, Matheson research grade, 99.999%; NH_3, Matheson anhydrous, 99.99%; CH_3OH, Sigma-Aldrich HPLC grade, 99.9%. HNCO is synthesized by a reaction of NaOCN powder (Aldrich Chemical 96%) with HCl gas (Aldrich Chemical 99+%), and purified with an ethanol/liquid nitrogen slush bath.

2.2. *UV Lamp Spectrum and Flux*

UV photons are provided by a microwave-powered (Opthos) hydrogen flow lamp. This is the same lamp used in Gerakines et al. (2000), and is similar to ones used in Allamandola et al. (1988), Gerakines et al. (1996), Ehrenfreund et al. (2001), and Baratta et al. (2002). The lamp is separated from the vacuum system by a lithium fluoride (LiF) window, transmitting $\lambda > 104$ nm. Lamp settings during irradiation are $P_{H_2} = 1000$ torr, microwave forward power 50%, reflected power less than 5%.

The UV spectrum of the lamp transmitted through the LiF window has been measured (with vacuum-pumped spectrometer Acton VM-502; detector Acton DA781) and is shown in Figure 1. This allows us to estimate that the average energy deposited during ice photolysis is $E = 7.41 \pm 0.23$ eV (average and uncertainty estimated from four successive spectra of the lamp emission). Lyα emission at 121.6 nm accounts for at most 5% of the total intensity between 100 and 200 nm.

The lamp flux has been measured using a calibrated NIST silicon photodiode. These flux measurements are compared to estimates of the flux obtained by measuring the $O_2 \rightarrow O_3$ conversion rate during the photolysis of a pure O_2 ice at 18 K.

2.2.1. *Photodiode Flux Measurements*

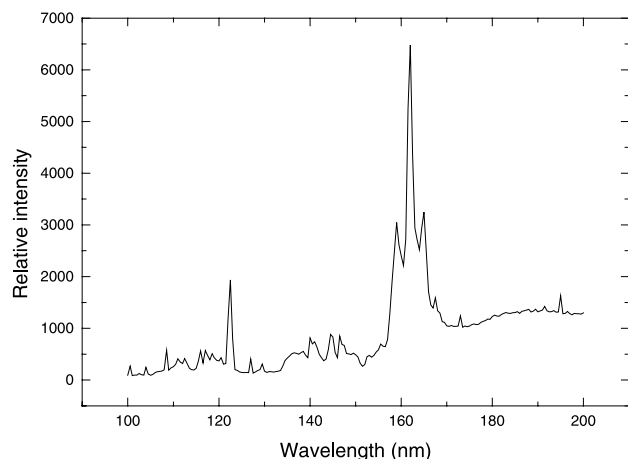Silicon photodiodes are broadband detectors that provide an absolute quantification of the flux emitted by the UV lamp. The photodiode is placed in the vacuum system at the location of the cold mirror, collecting exactly the same UV flux that would be received by an ice sample. The photon flux is calculated from the current produced by the photodiode, such as flux $= i/e$QE, where i is the current intensity, $e = 1.6 \times 10^{-19}$ coulomb electron^{-1}, and QE is the quantum efficiency of the photodiode in the 116–254 nm range. To estimate the evolution of the lamp flux as a function of time, two measurements have been performed separated by ∼60 hr of lamp utilization (times $t = 25$ and 88 hr with the same window). In addition, flux measurements have been performed for several microwave output powers; these fluxes are compared with oxygen ice actinometry.

2.2.2. *Oxygen Photolysis*

The actinometry method using O_2 ice photolysis to form O_3 is described in Gerakines et al. (2000). It is a well-documented method for gas-phase O_3 production (e.g., Warneck 1962). However, because of a lack of solid-phase data, gas-phase O_3 values are usually used, i.e., quantum yield of O_3 from O_2, QE = 1.92 (Groth 1937), and the strength of the O_3 stretching mode at 1040 cm^{-1}, $A = 1.4 \times 10^{-17}$ cm molecule^{-1} (Smith et al. 1985, p. 111). In our laboratory a pure O_2 ice is deposited. Its thickness is roughly 1.75 μm, which should allow a total absorption of the UV flux throughout the ice. But again, this estimation is based on a gas-phase absorption cross section (Okabe 1978) because of the lack of solid-phase data for O_2 in the vacuum UV. Therefore, we have checked that this method is not thickness dependent by comparing results obtained from both a 1.75 and a 3.25 μm ice. O_3 production is measured as a function of the time of photolysis, and the flux is derived from those measurements such as flux = [(Area under the 1040 cm^{-1} feature)/(photolysis time $\times$ QE $\times$ A)]. Actinometry experiments using these methods have been done for $t = 64$, 88, and 115 hr of lamp utilization. For $t = 88$ hr, measurements have been performed for several microwave output powers to be correlated with the photodiode results.

2.2.3. *Photodiode Flux Results Compared with Actinometry*

Table 1 shows the lamp flux, F, measured using the photodiode for different setting of the microwave generator compared to the flux obtained within the same conditions by O_2 photolysis. The use of gas-phase values for the QE and A-value do not give a flux equal to the calibrated value.

Fig. 1.—UV lamp spectrum, collected for $P_{H_2} = 1000$ torr, microwave forward power 50%, reflected power <4% (LiF window).

TABLE 1
Lamp Flux, F, Measured by a Photodiode and by
$O_2 \rightarrow O_3$ Actinometry

MICROWAVE SETTINGS FORWARD/ REFLECTED	F (photons s^{-1} cm^{-2})		
	Photodiode	Actinometry[a] QE $\times$ A = 2.69 $\times$ 10^{-17} cm photon^{-1}	Actinometry QE $\times$ A = 8.4 $\times$ 10^{-18} cm photon^{-1}
30/0	1.70×10^{14}	6.20×10^{13}	1.98×10^{14}
50/1	3.09×10^{14}	8.99×10^{13}	2.88×10^{14}
70/6	4.17×10^{14}	1.26×10^{14}	4.05×10^{14}
80/6	4.78×10^{14}	1.52×10^{14}	4.88×10^{14}

[a] $A = 1.4 \times 10^{-17}$ cm molecule^{-1}, QE = 1.92 molecule photon^{-1}

Ice thickness (μm)	F (photons s^{-1} cm^{-2})
1.75............................	$3.5 \pm 0.8 \times 10^{14}$
3.25............................	$3.4 \pm 0.8 \times 10^{14}$

Note.—We assumed QE $\times A = 8.4 \times 10^{-18}$ cm photon^{-1}. These experiments were not performed at the same time as the results presented in Table 1, which explains the difference between the fluxes. The forward/reflected setting was 50/2.

However, one must keep in mind that both the QE and A-value are subject to variations as a function of temperature and phase. Therefore, we propose to use a corrected value for QE $\times A$, which has been calculated in order to minimize $\Sigma(F_{O_2}^{\text{actinometry}} - F_{\text{photodiode}}^{\text{measured}})^2$: QE $\times A = 8.4 \times 10^{-18}$ cm photon^{-1}. This is nothing but a working value for actinometry measurements, which can be used in laboratories where a calibrated photodiode is not available, or for routine checks of the flux as photodiode measurements are more tedious to implement. The estimated uncertainty of the photon flux by O_2 photolysis is calculated by a least-square regression on $F_{\text{photodiode}}^{\text{measured}} = F_{O_2}^{\text{actinometry}}$ is $\pm 25\%$. Table 2 is a comparison of results for two ice thickness (1.75 and 3.25 μm), showing that O_2 results are not thickness dependent.

Figure 2 presents the evolution of the lamp flux as function of time. The decay is due to decreased transmission of the LiF window from the formation of yellow color centers. Those color centers can be removed by baking the window at about 300°C for a few hours. In this paper, photodestruction cross sections are calculated with a lamp flux estimated at the time of the experiment, from our measured linear regression of the actual flux due to the window's decreasing transmission. Again, uncertainty can be estimated to be $\pm 25\%$.
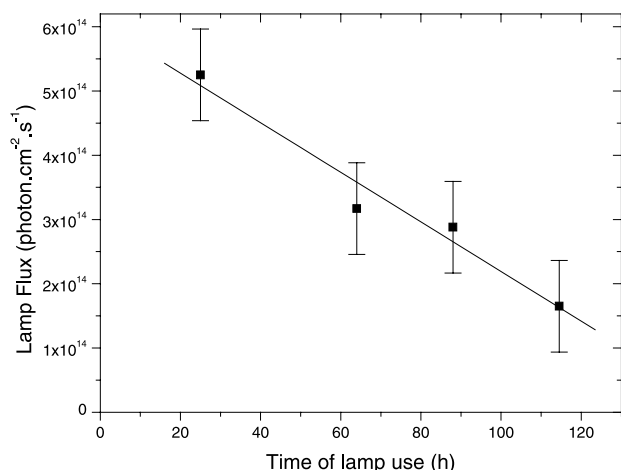

Fig. 2.—Evolution of the lamp flux as a function of time due to decreased transmittance of the LiF window.

3. SOME THEORETICAL ASPECTS OF ICE PHOTOLYSIS

The photodestruction of a molecule can be written as

$$AB \xrightarrow{h\nu} A^0 + B^0 ,$$

where AB is a molecule, and A^0 and B^0 are the resulting fragments. If N is the number density of AB (cm^{-3}), the photolysis rate is usually described by

$$\frac{dN}{dt} = -JN , \qquad (1)$$

where $J = \int_\lambda \sigma_\lambda I_\lambda \, d\lambda$, σ_λ being the destruction cross section of the molecule (cm^2), which is actually the product of the cross section of the molecule and the quantum yield of the photolysis reaction, and I_λ is the UV flux (photons s^{-1} cm^{-2}). Both σ and I are a function of the wavelength λ. If the ice is optically thin, then a first-order decay can be assumed and the value of J measured experimentally, as it is in Gerakines et al. (1996) and Ehrenfreund et al. (2001). The integrated form of equation (1) is

$$N(t) = N_0 \exp(-Jt) . \qquad (2)$$

Then the half-life, $t_{1/2}$, of the molecule [time for which $N(t) = N_0/2$] is written

$$t_{1/2} = \ln 2/J \qquad (3)$$

and does not depend on N_0. Here J is experimentally determined from the slope of a plot of $\ln N$ versus t for

$$\ln N = -Jt + \ln N_0 . \qquad (4)$$

Gerakines et al. (2000) assumed zeroth-order kinetics to calculate the destruction rate of CO_2 in H_2O ices and the production rate of CO and H_2CO_3. This is another analysis method for dealing with chemical reaction rates in which N is assumed to be constant and equal to N_0. The zeroth-order differential equation is

$$dN/dt = -JN_0 , \qquad (5)$$

and the integrated form is

$$N = N_0 - JN_0 t . \qquad (6)$$

Both equations (2) and (6) are equivalent, since as $t \rightarrow 0$ then $\exp(-Jt) \rightarrow (1 - Jt)$.

Equations (2) and (6) are no longer valid if the ice cannot be considered as optically thin, and thus the photon flux is not constant throughout the ice. In this case J is a function of the ice depth, as shown in Figure 3. Then, according to the Beer-Lambert law, neglecting diffusion within the ice,

$$J(z) = J_0 \exp(-Kz) , \qquad (7)$$

where J_0 is the J value at the top of the ice, z is the depth from the ice surface, and K is the absorption coefficient of the ice in cm^{-1}, assumed to be constant with depth and time.

Let us consider the ice sample as a succession of n layers in which J can be assumed to be constant (Fig. 3). Here N_1 to N_n are molecular number densities that are photolyzed at rates J_1 to J_n according to a first-order decay for each n layers; N_0 is the initial density of that molecule, and N is the average density in the ice for a time t of photolysis, as it would be measured, for example, by a spectrometer. The
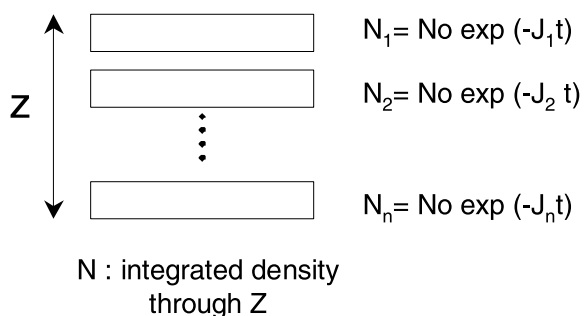
FIG. 3.—Schematic of ice sample seen as a succession of layers in which J can be assumed to be constant. Here N_1 to N_n are molecular number densities that are photolyzed at rates J_1 to J_n according to a first-order decay, N_0 is the initial density of that molecule, and N is the average density in the ice, as it would be measured, for example, by a spectrometer.
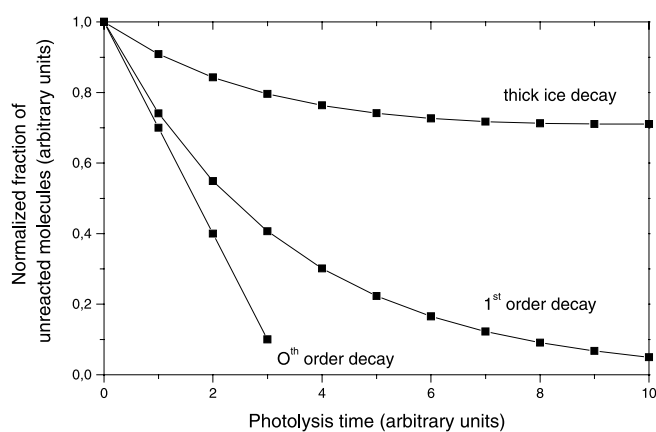

FIG. 4.—Comparison of the photodestruction rate of a molecule assuming zeroth or first-order kinetics in thin ice, and a first-order decay in thick ice. Densities are calculated from eqs. (2), (6), and (13) with the same J_0 absolute value.

average density N of a molecule AB being photolyzed in the ice can then be written

$$N = \frac{1}{n} \sum_{i=1}^{n} N_0 e^{-J_i t} \; , \qquad (8)$$

which yields, with Z being the ice thickness,

$$N = \frac{N_0}{Z} \int_0^Z e^{-J(Z)t} \, dz \; , \qquad (9)$$

and finally from equation (7),

$$N = \frac{N_0}{Z} \int_0^Z e^{-tJ_0 \exp(-Kz)} \, dz \; . \qquad (10)$$

If we write $A = tJ_0$ and $Y = \exp(-Kz)$, then equation (10) can be rewritten as

$$N = -\frac{N_0}{KZ} \int_1^{\exp(-Kz)} e^{-AY} \frac{dY}{Y} \; , \qquad (11)$$

where such an integration can be achieved knowing that

$$\int e^{ax} \frac{dx}{x} = \ln x + \frac{a\,x}{1!} + \frac{a^2 x^2}{2(2!)} + \frac{a^3 x^3}{3(3!)} + \cdots \; , \qquad (12)$$

which yields

$$N = N_0 \left\{ 1 + \frac{tJ_0}{KZ} \left[\sum_{i=1}^{n} \frac{(-tJ_0)^{i-1}}{i(i!)} \left(e^{-KZ} - 1 \right) \right] \right\} \; . \qquad (13)$$

From this equation, it appears necessary to quantitatively know both the ice thickness (Z) and absorption coefficient (K) to derive the actual photolysis rate J_0 and eventually the destruction cross section, σ, of the studied molecule. Figure 4 compares the normalized density decay rate for the three different equations according to zeroth- and first-order kinetics (eqs. [6] and [2]), and according to equation (13), for the same J_0 value.

One has to keep in mind that the absorption coefficient is a function of the wavelength, and that so far no ice photolysis experiments (including those presented in this paper) have been performed with a monochromatic UV lamp. This means that photons of different wavelengths reach different depths (Fig. 5) and that the J_0 and σ values derived from such experiments cover a range of wavelengths. Therefore,

extrapolation to interstellar environments must be done with caution.

Gerakines et al. (2000) calculated that the depth at which the UV transmission drops to 37% is 0.15 μm in water ice, based on a gas-phase water UV absorption cross section of 2×10^{-18} cm^2 (Okabe 1978). If one refers to Warren (1984) for hexagonal ice at 80 K and assumes $\rho = 1$ g cm^{-3}, the water ice absorption cross section is about 8×10^{-18} cm^2 between 115 and 155 nm, but drops down for higher wavelengths (see Fig. 5). (We have already shown that the UV lamp used for our experiments delivers photons ranging mainly from 120 to 180 nm.) For amorphous ice, such as the one we use in our experiments, the absorption cross section seems to be slightly lower than for hexagonal ice, but still within the same order of magnitude (Warren 1984, Fig. 1). Hence, for pure water ice, 10% of the UV flux below 155 nm is absorbed within the first 10^{-2} μm of the ice (Fig. 5) and 90% within 0.1 μm. Based on these data, H$_2$O ices 0.1–1 μm thick cannot be considered optically thin for Lyα, and instead of first-order fits, the more complicated analysis represented by equation (13) is required. Preparation of optically thin ice would experimentally be very difficult to
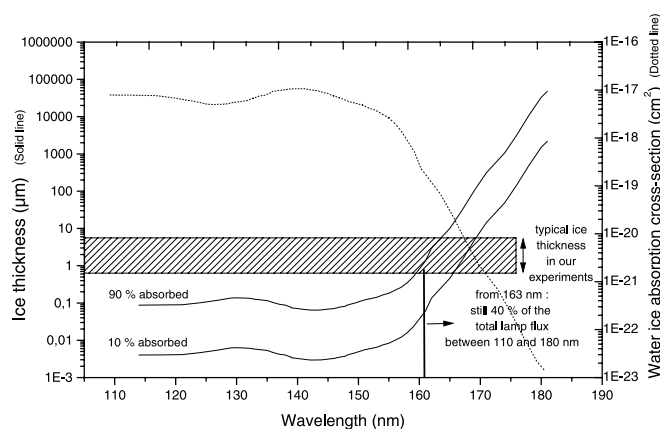

FIG. 5.—Ice thickness to which 10% and 90% of the UV flux is absorbed as a function of the wavelength (solid line). The absorption cross section of water ice calculated from Warren (1984) is also plotted (dotted line) as a function of wavelength.

achieve, and would result in weak spectral signatures which may not be sufficient for quantitative studies of photodestruction by infrared spectroscopy. Photons with lower energy than Lyα are nevertheless transmitted throughout the 0.1–1 μm thick laboratory ice (Fig. 5).

Photolysis experiments are performed on different kinds of ices (pure, mixed with water, N_2, or rare gas matrices); however, little is known about the optical properties of these ices or icy mixtures as a function of the wavelength in the far-UV. Baratta et al. (2002) measured some absorption coefficients at Lyα (but this is more likely an average value over the whole UV range of their lamp) at 12.5 K: H_2O (28×10^4 cm^{-1}), CH_4 (19×10^4 cm^{-1}), CH_3OH (12×10^4 cm^{-1}), or 8.4×10^{-18}, 5.7×10^{-18}, and 3.6×10^{-18} cm^2 molecule^{-1}, respectively, assuming an ice molecular density of 3.34×10^{22} molecules cm^{-3}. These coefficients are of the same order of magnitude, which means that our previous discussion about water ice can probably be extended to the other ices we have investigated, pure and mixed with water. In the gas phase, the N_2 absorption cross section is about 2×10^{-21} cm^2 in the far-UV (116–145 nm) (Okabe 1978), and if we assume the same order of magnitude in the solid phase, N_2 ices are transparent to UV photons above 116 nm, up to about 15 μm thickness. Thus, the molecules embedded in nitrogen ices are the main absorbers during photolysis, and compared to pure ices, the UV penetration depth in N_2 mixtures is enhanced by a factor equal to the dilution ratio of those molecules in nitrogen.

Yet, despite our discussion, we will see that results presented in this paper were fitted with first-order decay, as is the case for Gerakines et al. (1996, Fig. 13) and Ehrenfreund et al. (2001, Fig. 2). This can be explained by the fact that the microwave-powered hydrogen lamps used in such experiments produce a nonnegligible fraction of Lyα (121.6 nm) photons, and a large amount of photons at wavelengths above 160 nm (Fig. 1), for which ices can be considered as optically thin (Fig. 5). This might explain the first-order kinetics observed, and validate the reported J, σ, or half-life as long as one considers that values are integrated over the whole UV lamp emission spectrum, and not only at Lyα.

4. RESULTS AND DISCUSSION

The photostability of CH_4, CH_3OH, NH_3, CO_2, CO, and HNCO and mixtures of these molecules in N_2- and H_2O-rich ices were recorded using infrared spectra as a function of UV processing. The area of one of the dominant infrared peaks of each molecule was measured as a function of the processing time. The following bands were used: (C—H bend) CH_4 1300 cm^{-1}, (C—O st) CH_3OH 1017 cm^{-1}, (N—H bend) NH_3 1110 cm^{-1}, (C=O strecht) CO_2 2342 cm^{-1}, (C≡O strecht) CO 2137 cm^{-1}, and (C–N, C=O strecht) HNCO 2250 cm^{-1} (the actual position of the band may vary by a few cm^{-1} with the composition of the ice). No fit can be obtained between our experimental results and equation (13) by adjusting J_0, nor by adjusting Z or K within an order of magnitude around the value at which they are estimated. But as shown in Figure 6, plotting the logarithm of the normalized peak area as a function of time results in a linear decay, which shows that our ices are thin enough to be considered optically thin for most of the UV photons delivered by our lamp, as discussed in the previous section. This allows us to derive J according to equation (4) (the area being proportional to the number density of reactant mole-

cules in the ice), and the resulting destruction cross section $\sigma = J/I$ (I = lamp flux). This destruction cross section depends on the UV lamp emission spectrum, and is therefore an average value for photons ranging from 120 to 200 nm, with an average energy of 7.4 eV.

Figure 6 shows a linear first-order decay for roughly the first hour of photolysis, after which a non–first-order behavior sets in. This is most probably due to two main factors:

1. Further reactions occur in the ice including reproduction of the initial compound from reactions between its photoproducts.

2. Changes of the optical properties of the ice occur, because of the production of new compounds that enhance absorption of the lamp flux, leading to a decrease in photolysis efficiency with time. Such a phenomenon is reported in Khriachtchev, Pettersson, & Räsänen (1998).

The destruction cross section uncertainties are calculated as the sum of the relative uncertainty on J (estimated with a least-square regression on the experimental results) and the 25% uncertainty on the lamp flux.

A summary of our results is given in Table 3. For pure ices, our results are of the same order of magnitude as those published by Gerakines et al. (1996), except that ours are systematically lower by a factor of 2–7. A consistent explanation for this trend would be that the UV flux used in the Gerakines paper was underestimated (actually, the flux was not exactly known but was assumed to be 10^{15} photons s^{-1} cm^{-2}), or if the emission spectrum of the lamp was slightly different from ours in the far-UV.

For each molecule, a half-lifetime can then be estimated in the diffuse interstellar medium (assuming an interstellar flux of 10^8 photon cm^{-2} s^{-1} for photons greater than 6 eV; Mathis, Mezger, & Panagia 1983), and in dense molecular clouds (assuming a cosmic-ray–induced UV flux of 10^3 photons cm^{-2} s^{-1}; Prasad & Tarafdar 1983). These half-lives, such as the ones presented in this paper or in Ehrenfreund et al. (2001), should be considered as kinetic values related *only* to photodestruction sinks for the molecules in simple ice mixtures. For example, one should not assume that in the diffuse ISM, the number density of CH_4 in H_2O ice is divided by 2 within 1471 yr. In the presence of other reactants representing a more relevant complex interstellar-type mixture, CH_4 is also produced (for example from photolyzed H_2O + CH_3OH ices [Allamandola et al. 1988; Bernstein et al. 1995], or from ion-irradiated H_2O + CO ices [Moore, Khanna, & Donn 1991]), and its concentration results from the balance between sinks and sources.

During photolysis, the intensity of the CO absorption does not measurably decrease if it is in pure form or mixed with nitrogen, e.g., N_2 + CO (10 : 1). For those two experiments we have derived an upper limit for the half-life. One of the most interesting points is that CO is clearly destroyed when mixed with H_2O. By itself, CO is not photodissociated for wavelengths above 112 nm (Okabe 1978). Nevertheless, as already reported by Gerakines et al. (1996), some CO_2 or other products are synthesized in reactions of its excited state,

$$CO + h\nu \rightarrow CO^* \, ,$$

$$CO^* + CO \rightarrow CO_2 + C \, .$$
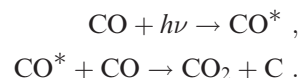
The fact that no significant CO_2 production is observed in the N_2 + CO (10 : 1) experiment is consistent with this mechanism, since CO is isolated in this N_2 matrix.

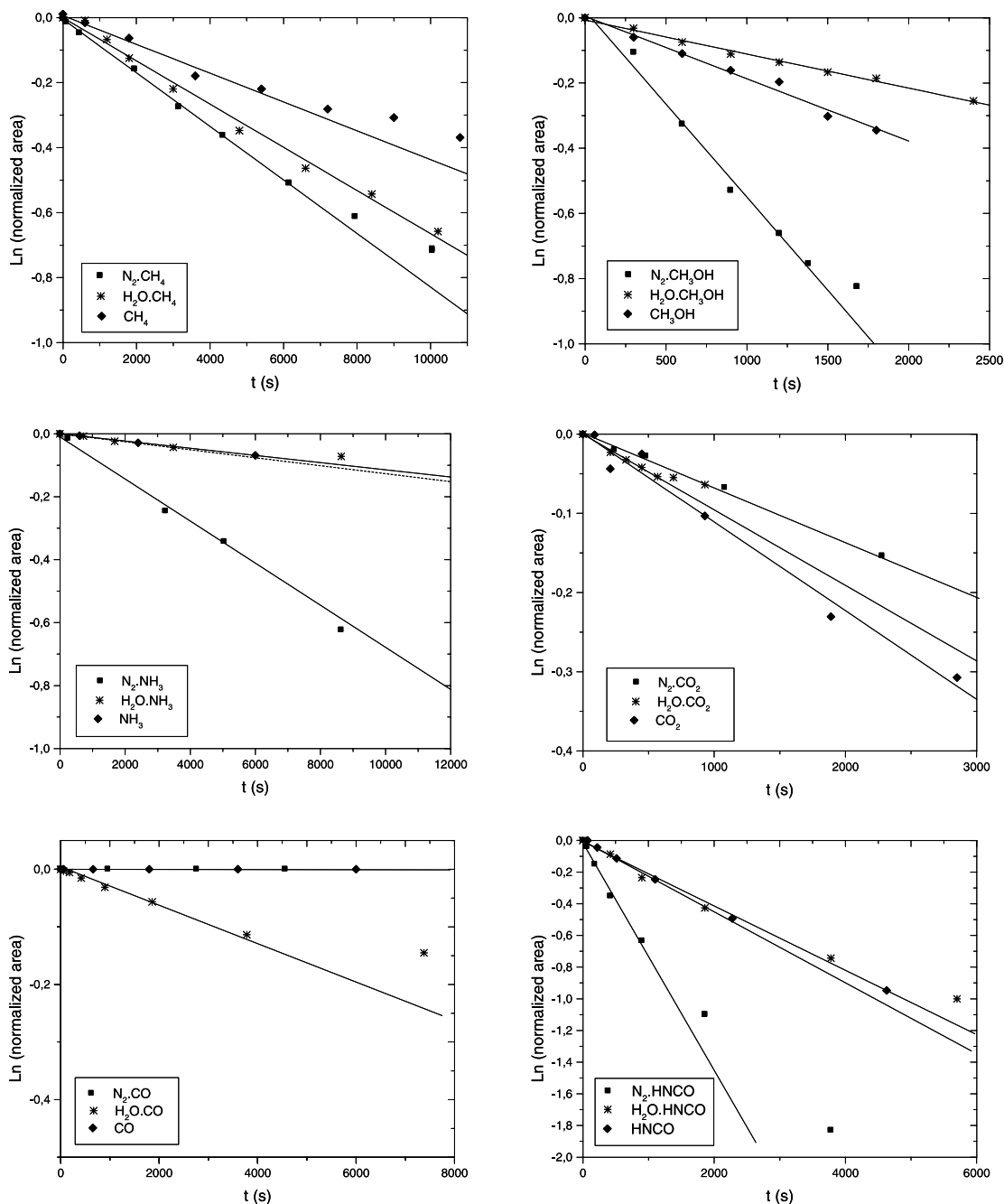Fig. 6.—Experimental results show decreases in normalized IR band area as a function of photolysis time. Results for CH_4, CH_3OH, NH_3, CO_2, CO, and HNCO, as pure ices and mixed with H_2O or N_2, assume first-order decay kinetics. The following IR bands were used: CH_4 1300 cm^{-1}, CH_3OH 1017 cm^{-1}, NH_3 1100 cm^{-1}, CO_2 2342 cm^{-1}, CO 2137 cm^{-1}, and HNCO 2250 cm^{-1}.

When mixed with H_2O, if one refers to the gas-phase chemistry, CO can react with OH, a product of water photolysis (Atkinson et al. 1997),

$$H_2O + h\nu \rightarrow OH + H \ ,$$
$$OH + CO \rightarrow CO_2 + H \ .$$
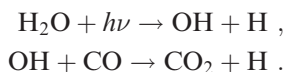
This explains the dramatic change observed in CO, in the presence or absence of H_2O. Hence, σ depends not only on the photodestruction cross section of CO, but also on its reactivity with other photolysis products.

A similar increase in destruction rates in H_2O is not observed for the other molecules studied, even though gas-

phase reactions with OH are reported for CH_4, CH_3OH, NH_3 (Atkinson et al. 1997), and HNCO (Wooldridge, Hanson, & Bowman 1996), leading to the abstraction of an H. Such reactions do not appear to be as significant, compared to direct photodissociation.

For CH_4, CH_3OH, NH_3, and HNCO, destruction is faster in N_2. In such ices, only pure photodissociation processes are likely to happen, since molecules are isolated from each other in the N_2 matrix (N_2 is not dissociated and is transparent at our wavelengths). The slower decay of pure ices or water-dominated ices could be due to competition between the actual molecule photolysis, such as observed in nitrogen, with other reactions in a more complex chemical

TABLE 3
DESTRUCTION CROSS SECTION OF MOLECULES MEASURED IN THIS WORK COMPARED TO PREVIOUSLY PUBLISHED VALUES

Ice	Ice Mixture Ratio	σ (This Work) (cm^2)	Relative Uncertainty (This Work) (%)	σ (Gerakines et al. 1996) (cm^2)	Half-life (y) Diffuse ISM	Half-life (10^6 years) Dense IS Cloud
CH$_4$	pure	9.1×10^{-20}	31	7.2×10^{-19}	2407	241
CH$_4$: N$_2$	1 : 10	1.8×10^{-19}	29		1218	122
CH$_4$: H$_2$O	1 : 10	1.5×10^{-19}	33		1471	147
CH$_3$OH..............	pure	5.0×10^{-19}	39	1.6×10^{-18}	442	44
CH$_3$OH : N$_2$	1 : 10	1.5×10^{-18}	38		148	15
CH$_3$OH : H$_2$O	1 : 10	2.7×10^{-19}	33		807	81
NH$_3$	pure	3.2×10^{-20}	32		6952	695
NH$_3$: N$_2$	1 : 10	2.3×10^{-19}	35		937	94
NH$_3$: H$_2$O	1 : 10	4.8×10^{-20}	54		4531	453
CO$_2$....................	pure	3.8×10^{-19}	41	5.6×10^{-19}	584	58
CO$_2$: N$_2$	1 : 10	2.6×10^{-19}	29		845	85
CO$_2$: H$_2$O	1 : 10	3.3×10^{-19}	35		657	66
CO......................	pure	$<1 \times 10^{-21}$	...	$<8 \times 10^{-20}$	>220,000	∞
CO : N$_2$	1 : 10	$<1 \times 10^{-21}$	...		>220,000	∞
CO : H$_2$O.............	1 : 10	1.2×10^{-19}	30		1894	189
HNCO..............	pure	6.9×10^{-19}	30		318	32
HNCO : N$_2$	1 : 10	2.5×10^{-18}	42		87	9
HNCO : H$_2$O	1 : 10	7.1×10^{-19}	39		312	31

NOTE.—Prediction of photodestruction half-life in both diffuse interstellar medium, and dense interstellar clouds based on our work.

system. For CO$_2$, no significant difference can be noted between the three experiments, which provides good information on its destruction cross section regardless of the composition of the bulk of the ice in which it is embedded.

Baratta et al. (2002) state that the destruction rate in such experiments cannot be extrapolated for a high-energy dose. We think that even if the observed destruction rate changes with time, σ is constant and a pertinent parameter to derive from such experiments. The change in an ice's absorption coefficient should be taken into account when modeling the composition of a photolyzed ice, since the photolysis rate, J, is the product of σ (constant) and I (UV flux, which may change with depth and time as the ice composition changes). For high-energy doses, sources and sinks have to be taken into account. Data derived from the linear section of our results are only related to sinks of the studied molecules, which might also be regenerated through reactions of their products.

Our results are a step toward a compilation of photochemical data that should allow modeling of the composition of interstellar ices over long periods of time. An interesting result of our work is the destruction rate dependence on ice environment. As discussed earlier in this paper, more work is still needed, and particularly work concerning knowledge of the ice absorption coefficient in the far-UV and its dependence with wavelength. Moreover, the σ values estimated from our work cover a large wavelength range, and further work should now focus on monochromatic studies. For example, 122 nm dominant emission can be achieved with a microwave-powered lamp using an H$_2$-He mixture, 147 nm with xenon, etc. (Cottin et al. 2000; Okabe 1978). Such data will be necessary for an accurate description of interstellar ice chemistry.

REFERENCES

Allamandola, L. J., Sandford, S. A., & Valero, G. J. 1988, Icarus, 76, 225
Atkinson, R., Baulch, D. L., Cox, R. A., Hampson, R. F., Jr., Kerr, J. A., Rossi, M. J., & Troe, J. 1997, J. Phys. Chem. Ref. Data, 26, 1329
Baratta, G. A., Leto, G., & Palumbo, M. E. 2002, A&A, 384, 343
Bernstein, M. P., Sandford, S. A., Allamandola, L. J., Chang, S., & Scharberg, M. A. 1995, ApJ, 454, 327
Boogert, A. C. A., Helmich, F. P., van Dishoeck, E. F., Schutte, W. A., Tielens, A. G. G. M., & Whittet, D. C. B. 1998, A&A, 336, 352
Cottin, H., Gazeau, M. C., Doussin, J. F., & Raulin, F. 2000, J. Photochem. Photobiol., 135, 53
Cottin, H., Gazeau, M. C., & Raulin, F. 1999, Planet. Space Sci., 47, 1141
Dworkin, J. P., Deamer, D. W., Sandford, S. A., & Allamandola, L. J. 2001, Proc. Natl. Acad. Sci., 98, 815
Ehrenfreund, P., Bernstein, M. P., Dworkin, J. P., Sandford, S. A., & Allamandola, L. J. 2001, ApJ, 550, L95
Ehrenfreund, P., d'Hendecourt, L., Dartois, E., de Muizon, M. J., Breitfellner, M., Puget J. L., & Habing, H. J. 1997, Icarus, 130, 1
Gerakines, P. A., & Moore, M. H. 2001, Icarus, 154, 372

Gerakines, P. A., Moore, M. H., & Hudson, R. L. 2000, A&A, 357, 793
Gerakines, P. A., Schutte, W. A., & Ehrenfreund, P. 1996, A&A, 312, 289
Gerakines, P. A., et al. 1999, ApJ, 522, 357
Gibb, E. L., et al. 2000, ApJ, 536, 347
Groth, W. 1937, Zeitschr. Phys. Chemie, 37, 307
Hudson, R. L., & Moore, M. H. 1995, Radiat. Phys. Chem., 45, 779
———. 1999, Icarus, 140, 451
Jackson, J. M., Armstrong, J. T., & Barrett, A. H. 1984, ApJ, 280, 608
Khriachtchev, L., Pettersson, M., & Räsänen, M. 1998, Chem. Phys. Lett., 299, 727
Lacy, J. H., Faraji, H., Sandford, S. A., & Allamandola, L. J. 1998, ApJ, 501, L105
Lis, D. C., et al. 1997a, Icarus, 130, 355
———. 1997b, Earth Moon Planets, 78, 13
Mathis, J. S., Mezger, P. G., & Panagia, N. 1983, A&A, 128, 212
Moore, M. H., & Hudson, R. L. 1998, Icarus, 135, 518
———. 2000, Icarus, 145, 282
Moore, M. H., Khanna, R., & Donn, B. 1991, J. Geophys. Res., 96, 17541

Okabe, H. 1978, Photochemistry of Small Molecules (New York: Wiley-Interscience)

Prasad, S. S., & Tarafdar, S. P. 1983, ApJ, 267, 603

Schutte, W. A., Allamandola, L. J., & Sandford, S. A. 1993, Icarus, 104, 118

Smith, M. A. H., Rinsland, C. P., Fridovich, B., & Rao, K. N. 1985, Molecular Spectroscopy: Modern Research, Volume 3 (London: Academic Press)

Snyder, L. E., & Buhl, D. 1972, ApJ, 177, 619

Warneck, P. 1962, Appl. Opt., 1, 721

Warren, S. G. 1984, Appl. Opt., 23, 1206

Watanabe, N., & Kouchi, A. 2002, ApJ, 567, 651

Wooldridge, M. S., Hanson, R. K., & Bowman, C. T. 1996, Int. J. Chem. Kinetics, 28, 361